Exp Brain Res (2005) 163: 44–57
DOI 10.1007/s00221-004-2137-1

RESEARCH ARTICLE

Dmitry Domkin · Jozsef Laczko · Mats Djupsjöbacka
Slobodan Jaric · Mark L. Latash

Joint angle variability in 3D bimanual pointing: uncontrolled manifold analysis

Received: 25 March 2004 / Accepted: 2 October 2004 / Published online: 25 January 2005

Abstract The structure of joint angle variability and its changes with practice were investigated using the uncontrolled manifold (UCM) computational approach. Subjects performed fast and accurate bimanual pointing movements in 3D space, trying to match the tip of a pointer, held in the right hand, with the tip of one of three different targets, held in the left hand during a pre-test, several practice sessions and a post-test. The prediction of the UCM approach about the structuring of joint angle variance for selective stabilization of important task variables was tested with respect to selective stabilization of time series of the vectorial distance between the pointer and aimed target tips (bimanual control hypothesis) and with respect to selective stabilization of the endpoint trajectory of each arm (unimanual control hypothesis). The components of the total joint angle variance not affecting (V_{COMP}) and affecting (V_{UN}) the value of a selected task variable were computed for each 10% of the normalized movement time. The ratio of these two components $R_V = V_{COMP}/V_{UN}$ served as a quantitative index of selective stabilization. Both the bimanual and unimanual control hypotheses were supported, however the R_V values for the bimanual hypothesis were significantly higher than those for the unimanual hypothesis applied to the left and right arm both prior to and after practice. This suggests that the CNS stabilizes the relative trajectory of one endpoint with respect to the other more than it stabilizes the trajectories of each of the endpoints in the external space. Practice-associated improvement in both movement speed and accuracy was accompanied by counter-intuitive lack of changes in R_V. Both V_{COMP} and V_{UN} variance components decreased such that their ratio remained constant prior to and after practice. We conclude that the UCM approach offers a unique and under-explored opportunity to track changes in the organization of multi-effector systems with practice and allows quantitative assessment of the degree of stabilization of selected performance variables.

Keywords Uncontrolled manifold · Variability · Voluntary movement · Coordination · Synergy

D. Domkin (✉) · M. Djupsjöbacka
Centre for Musculoskeletal Research,
University of Gävle,
Box 7629, 907 12 Umeå, Sweden
E-mail: dmitry.domkin@hig.se
Fax: +46-90-106099

D. Domkin
Department of Surgical and Perioperative Sciences,
Sports Medicine Unit, Umeå University,
901 87 Umeå, Sweden

J. Laczko
Department of Biomechanics, Semmelweis University,
1123 Budapest, Hungary

S. Jaric
Department of Health, Nutrition and Exercise Sciences,
University of Delaware, DE 19716, USA

M. L. Latash
Department of Kinesiology, The Pennsylvania State University,
University Park, PA 16802, USA

Introduction

The term "synergy" has been frequently used in the motor control literature in relation to the famous problem of motor redundancy (Bernstein 1967; Turvey 1990; Latash 1996): How does the central nervous system (CNS) select particular solutions for motor tasks, which typically have an apparently infinite number of ways to satisfy task requirements? Following the original ideas of Bernstein, a predominant approach has been that the CNS uses sets of pre-existent synergies that eliminate redundant degrees of freedom (DFs) by adding constraints (Vereijken et al. 1992; Piek 1995) or satisfy certain optimization criteria (reviewed in Seif-Naraghi and Winters 1990; Latash 1993; Rosenbaum et al. 1995). An alternative idea originated from seminal works by Gelfand and Tsetlin (1966) who suggested that the CNS always used all the DFs and organized them in flexible

task-specific structural units each time a movement is performed, even over repetitions of apparently the same motor task. These organizations have been assumed to facilitate stable performance with respect to important task variables (cf. the notion of ''coordinative structures'', Kugler et al. 1980).

In line with the latter idea, a computational method has been developed recently, named the uncontrolled manifold (UCM) approach (Scholz and Schoner 1999; Scholz et al. 2000; Latash et al. 2002). The UCM approach assumes that the controller acts in the state space of independent elemental variables and creates in that space a sub-space (a UCM) corresponding to a value of an important performance variable that needs to be stabilized. Then, the controller limits the variability of the elemental variables in directions orthogonal to the UCM more than within the UCM. The UCM approach has been successfully applied to studies of whole-body actions (Scholz and Schoner 1999; Reisman et al. 2002), multi-finger force production (Latash et al. 2001; Scholz et al. 2002) and multi-joint limb movements (Domkin et al. 2002; Tseng et al. 2003). It has also been used to discover and quantify atypical synergies in neurological patients, persons with Down syndrome and healthy elderly subjects (Reisman and Scholz 2003; Scholz et al. 2003; Shinohara et al. 2003).

Until now, the UCM approach has been applied to systems with relatively small number of explicitly involved elements (joints within one arm, fingers within one hand, etc.). Also, for computational purposes, many of the cited studies constrained the tasks to either isometric conditions or planar motion. In everyday life, most tasks involve several effectors of the body that act in a coordinated manner in the three-dimensional space. One purpose of the current study was to analyze the applicability of the UCM analysis to tasks that involve many joints across two effectors acting in a relatively unconstrained manner.

An attractive feature of the UCM approach is that it allows monitoring of the process of emergence of multi-effector synergies or of their refinement with practice. Until now, only a few studies applied this method to analyze changes in the coordination of elements with practice (Domkin et al. 2002; Latash et al. 2003; Kang et al. 2004). The results of these studies were ambiguous. In the study of the effects of practice on joint coordination during planar bimanual pointing by Domkin et al. (2002), an improvement of the performance was associated with a drop in the UCM effect (i.e. the variance within the UCM sub-space decreased more than that within the orthogonal sub-space) quantified as the ratio of variances computed in the joint angle space within and orthogonal to the UCM per DF. This finding was interpreted as a consequence of a floor effect because of the relative simplicity of the task that allowed the elaboration of a family of stereotypical trajectories. Two other studies used the task of isometric multi-finger force production. Within a relatively simple task, Latash et al. (2003) observed changes in the finger force variance suggesting an increase in the UCM effect (i.e. the variance within the orthogonal sub-space decreased more than that within the UCM sub-space) during the first phase of practice (about 100 trials over about 40 min) followed by a drop in the UCM effect over the second phase of practice (100 more trials). The study by Kang et al. (2004) used a very complex bimanual multi-finger force production task and showed that two days of practice led to an increase in the UCM effect characterizing finger interaction within each of the hands. However, there were no changes in the UCM effect with respect to the interaction of all involved fingers of both hands. Hence, another purpose of the current study was to observe practice-related changes in the UCM effect in a relatively complex task that would make it much more difficult for the participants to generate stereotypical solutions.

Control hierarchies have been frequently invoked in motor control theories starting from seminal works by Bernstein (1935, 1967). One recent example is the control of forces produced by the digits of the human hand in prehensile tasks. Two hierarchical levels have been hypothesized to participate in the control of prehension (MacKenzie and Iberall 1994). At the upper level, the required mechanical action was distributed between the thumb and the virtual finger, an imaginable finger, whose mechanical effect was equivalent to that of the four fingers of the hand. At the lower level, the action of the virtual finger was distributed among the actual fingers. This idea has received support in several recent studies (Baud-Bovy and Soechting 2001, 2002; Shim et al. 2003). We may expect that bimanual actions also can be controlled as a hierarchy. In our previous study (Domkin et al. 2002) we found that the CNS stabilized the synergy of two arms (higher hierarchical level of control) to larger degree than it did for the coordination between joints of each arm separately (lower hierarchical level of control).

To address these issues, we studied the coordination of joints within each arm and between arms during a two-hand pointing task involving one pointer and three targets. The UCM analysis was applied to joint angle data recorded in blocks of trials. Note that such analysis requires computation of a UCM with respect to a value of a performance variable, which is presumably stabilized by the CNS. That is, it always starts with the formulation of a hypothesis that elemental variables (joint angles) covary to preserve a value of a particular variable. We will address these as ''control hypotheses'' (cf. Scholz et al. 2000; Latash et al. 2002).

We analyzed two control hypotheses in this study. One of them implies that at each phase of the trajectory joint angles within an extremity covary to preserve the average position of the arm endpoint. This hypothesis is denoted the ''unimanual'' control hypothesis and is applied separately to the left and right arm. Panel A of Fig. 1 illustrates three joint configurations that all belong to the same UCM computed with respect to the unimanual control hypothesis applied to the right arm, since they aim towards the same final spatial position.

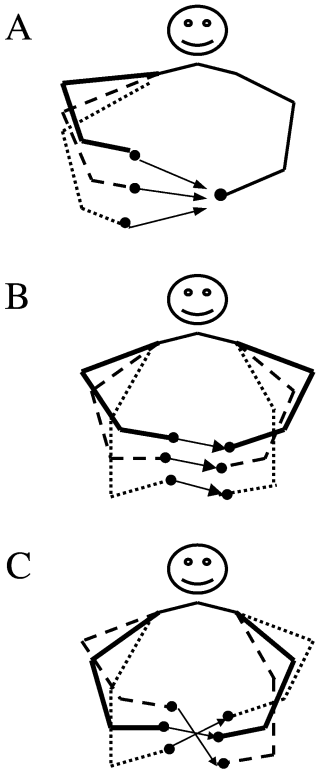

Fig. 1 Illustration of the bimanual and unimanual control hypotheses. **A**: unimanual hypothesis applied to the right arm confirmed; **B**: bimanual hypothesis confirmed; **C**: bimanual hypothesis rejected

Our previous study (Domkin et al. 2002) has suggested that the two-arm coordination in a bimanual pointing task is not simply a superposition of two single-arm synergies, but that joint angles covary across the arms as well. To test this possibility in the current study, we considered a two-arm control hypothesis, illustrated in Panel B of Fig. 1. The hypothesis assumes that joint angles of the two arms covary to stabilize the vectorial distance between the pointer and the aimed target tips (''bimanual'' control hypothesis). Panel C of Fig. 1 illustrates a situation when deviations of the endpoints of the two arms do not covary and hence do not comply with the bimanual control hypothesis.

This study addresses three main predictions. First, we hypothesize that the general principle of UCM control will be applicable to relatively unconstrained multi-effector motor tasks. The second prediction is that an increase in task complexity (compared with the previous study, Domkin et al. 2002) would eliminate the decrease of the UCM effect with practice and may even be associated with an increase of this effect. The third prediction is that when the task becomes complex and involves the coordination of many joints, the CNS may use a hierarchical control reflected in different degrees of stabilization of important performance variables by different subsets of effectors. Thus, we expect that the CNS would primarily stabilize the relative position of the endpoints of two arms, as required by the nature of the task, showing a synergy between arms in line with the bimanual control hypothesis. At the same time the CNS may or may not use within-an-arm multi-joint synergies to stabilize each effector's endpoint trajectory. That is, the unimanual control hypothesis may or may not be supported.

Methods

Subjects

Ten healthy female university students (age 22.8 ± 1.3 years, height 164.5 ± 4.6 cm and body mass 62 ± 4.7 kg; Mean $\pm$ SD) participated in the study. All subjects were right-handed and without neurological diseases, recent injuries or musculoskeletal problems in the neck, shoulder, arm or hand regions. The subjects received verbal and written descriptions of all procedures and the tests were performed after an informed consent had been signed. The study was approved by the Ethical Committee of the Medical Faculty of the Umeå University and was performed in accordance with the ethical standards laid down by the Declaration of Helsinki in 1964.

Apparatus

The subjects sat in a rigid chair, with their torso and shoulders tightly strapped, with wide belts, to the back of the chair. The belts restricted movements in the torso and the clavicular joints, allowing free movements in the shoulder joints. Height-adjustable supports for the arms in the starting position were located on both sides of the chair (Fig. 2A).

Rectangular plastic plates were firmly attached to the subjects' palms, such that the digits were extended, adducted and no movements were possible in the joints distally to the wrist. A pointer was attached to the right hand plate, while three pointers were attached to the left hand plate (see Fig. 2C for illustration of both the shape and size). We will denote the left-hand pointers as ''targets'', while the right hand one will be called ''pointer''. The masses of the entire left and right hand devices were 210 and 160 g, respectively.

Data collection

Kinematic data for both arms were recorded by means of two synchronized electromagnetic tracking systems (Fastrak, Polhemus, USA), one system used for each arm. Each system recorded movements of four sensors by tracking their 3D position and orientation at a sampling rate of 30 Hz. The sensors were firmly placed on the skin on the following locations of each arm: the shoulder on top of the acromion; the dorsal surface of the upper arm, approximately 5 cm from the elbow joint; the dorsal surface of the forearm, approximately 2 cm from the wrist

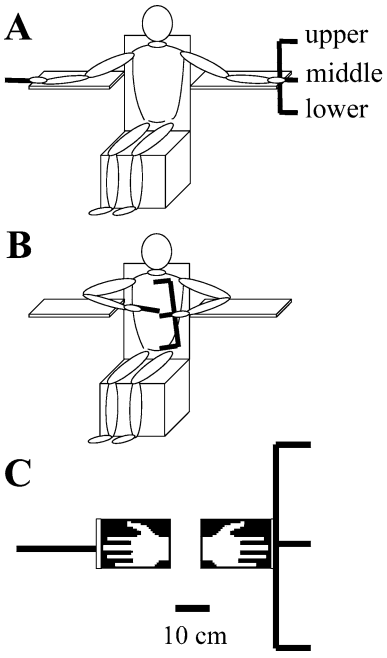

Fig. 2 Experimental conditions. **A**: starting position; **B**: position at the instant of movement termination; **C**: left and right hand pointer devices

joint; the plastic plate attached to the hand, approximately on the level of the proximal end of the metacarpus.

Power spectral analysis of the pointing movement data (averaged across trials, subjects, arms and tests) showed that for all data (coordinates and angles) 99% of the power was located in the frequencies below 1.1 Hz, indicating that the sampling rate of 30 Hz was sufficient.

Testing and practice procedure

The three left-hand pointers were denoted "upper", "middle" and "lower" according to their location in the initial position of the left arm (Fig. 2A). Thus, pointing was performed with the right hand pointer to the upper, middle or lower target (Fig. 2B). On a command containing the name of the aimed target the subjects were instructed to perform a fast and accurate pointing movement matching the pointer tip with the tip of the aimed target. There were no instructions regarding any point in space where the pointer and target tips should meet. A trial (i.e. pointing movement) was completed when the 3D velocity of the sensors attached to both hand plates dropped below 0.5 cm s^{-1}. Analysis of pilot data showed that this limit optimally separated the final stationary phase of the pointing movement from subsequent random movements.

Experimental design

The subjects performed a pre-test on the first day, followed by a practice session on the same day. Two more practice sessions were performed on the second day and, finally, a post-test on the third day. The sessions of one day were separated in time by at least three hours. The movements to different targets were performed in a pseudo-random order. All movements were separated into blocks of 20 trials by pauses of approximately two minutes. The pre-test and post-test consisted of 60 trials each (i.e. 20 pointing movements to each target). In the pre-test and post-test the subjects were blindfolded all the time during pointing movements, except during the pauses, when they were asked to perform one pointing movement to each target with vision. The practice sessions consisted of 120 trials each (40 pointing movements to each target). In the practice sessions the subjects had their eyes closed during pointing movements. The subjects were instructed to open their eyes after the completion of each movement and look at the final positions of the pointer and aimed target tips.

Data processing

The kinematic data for both arms were represented in a common global coordinate system with the origin in the supra-sternal notch. The global coordinate system had an orientation such that its coordinate axes X, Y and Z corresponded to the medial–lateral, ventral–dorsal and vertical directions in relation to the body, respectively. The coordinate values for the X, Y and Z axes increased with the movement progressing to the right, forward and upward in relation to the body, respectively.

Computation of joint angles

A three-segment rigid-body model was used for calculation of the joint angles. The model included upper arm, forearm and hand segments. All segments were assumed coupled such that the end of one segment also represented the beginning of an adjacent segment. The shoulder joint angles were represented in the global coordinate system and included horizontal abduction–adduction, flexion–extension and inward–outward rotation. The angles of the elbow and wrist joints were represented in local coordinate systems such that the coordinate system of a proximal segment was a base for a corresponding coordinate system of the adjacent distal segment. The angles of the elbow joint were flexion–extension, abduction–adduction (anatomically restricted) and forearm pronation–supination. The angles of the wrist joint were flexion–extension, abduction–adduction and hand pronation–supination (anatomically restricted). The hand segment started from the distal end of the forearm segment and ended at either the pointer or target tip. Therefore, three separate left hand segments were used, depending upon the aimed target.

We performed calibration of the placement of the sensors prior to each testing and practice session. First, approximate coordinates of the arm segments' endpoints

were collected with a separate Fastrak stylus-sensor. Then, the subject performed a movement utilizing all degrees of freedom and full range of joint motion in both arms. Using the approximate coordinates of the arm segments' endpoints and data from the sensors, placed on the arm segments, we computed preliminary calibration data describing the location and orientation of each sensor relative to its segment. Thereafter, we applied an algorithm to obtain optimized calibration data describing the location and orientation of each sensor relatively to its segment (Djupsjöbacka et al. 1999). The presumption for this algorithm was that the distance between the ends of adjacent segments in each joint (''joint distance'') should be zero. Thus, the algorithm provided optimized calibration data and coordinates of the segments' endpoints by minimizing the joint distances. In the calibrated segment model the averaged across trials, subjects, arms and tests joint distance was 1.6 ± 0.3, 3.0 ± 0.7 and 0.8 ± 0.4 cm (mean $\pm$ SD) for the shoulder, elbow and wrist joints, respectively.

For computation of the joint angles we used orientation angles (azimuth, elevation and roll) of the Fastrak sensors attached to the arm segments. The matrices for the rotations around axes X, Y and Z were the standard rotation matrices (Anton and Rorres 2000). The resulting rotation matrix ${}^{G}R_{S}$ from the sensor's base (subscript ''S'') to the global reference frame (''G'') was equivalent to the product of multiplication of the standard rotation matrices describing rotations of the sensor around the global axes $R_Z{*}R_Y{*}R_X$. Using the optimized calibration data describing the orientation of the sensor relative to its segment we obtained for each segment a transformation matrix ${}^{S}R_{SEG}$ from the segment's base (''SEG'') to the sensor's base. The rotation matrix for the shoulder joint relative to the global reference frame had a general form ${}^{G}R_{SEG} = {}^{G}R_{S}{*}{}^{S}R_{SEG}$, where ''SEG'' represented the humerus segment. The rotation matrices for the elbow and wrist joints were obtained as $[{}^{G}R_{SEG1}]^{T}{*}{}^{G}R_{SEG2}$, where ''T'' stands for the transpose and ''SEG1'' and ''SEG2'' for the adjacent proximal and distal segments, respectively. Then, Euler angles were obtained from the rotation matrices for each joint.

An additional algorithm was applied for calculation of the shoulder inward–outward rotation and elbow joint angles (Djupsjöbacka et al. 1999). This algorithm allowed for errors due to skin sliding below the upper arm sensor during inward–outward rotations of the humerus. The presumption for this algorithm was that the anatomically restricted elbow abduction–adduction should be zero. Hence, the upper arm rotation was adjusted for each sample such that the elbow abduction–adduction angle was minimized. The data processing and computations were performed with Matlab 5.3 (The MathWorks).

Kinematic variables

Movement initiation and termination were assessed for each arm separately from the velocity profiles of the pointer and aimed target tips. The initiation corresponded to the instant when the velocity of the pointer or target tip exceeded 10% of its maximal value. The termination corresponded to the instant when the velocity dropped below the same value. Pilot data analysis revealed that the 10% limit of the maximum velocity optimally separated the dynamic part of the pointing movement trajectory from its terminal phase. The same analysis also showed that there were no significant differences in the initiation and termination time between the arms. Nevertheless, the movement time of each particular trial was calculated from the earlier initiation to the later termination time.

The length of the trajectory of the shoulder joint center during the movement (averaged across trials, subjects, arms and tests) was 3.16 ± 0.7 cm (mean $\pm$ SD). This finding suggests that the motion of the torso and clavicular joints taken together was sufficiently constrained by the straps.

Analysis of pilot data revealed that the positions of the pointer and aimed target tips remained virtually stationary approximately 500 ms after the end of the movement time. Therefore, both the accuracy and the meeting point location were assessed at this instant, which will be denoted ''movement termination''.

The overall accuracy of the pointing movement was assessed as the scalar distance between the pointer and aimed target tips at the instant of movement termination. The variability of the pointer tip position relative to the tip of the aimed target (variable error) was calculated along each coordinate axis as the standard deviation of the detrended differences between the locations of the pointer and aimed target tips. The meeting point was defined as the midpoint of the line connecting the final positions of the pointer and aimed target tips at the instant of movement termination. The variability of the meeting point was computed along each coordinate axis as the standard deviation of the detrended meeting point coordinates of individual trials. The velocity of the pointer and aimed target tips and of the scalar distance between them was computed as the first derivative of the coordinate data with application of a low pass 4th order Butterworth filter with a cut-off frequency of 3 Hz.

Computation of total joint variance

The total variance in joint space V_{TOT} was computed from 20 sequential pointing movements, performed to each target. Angular trajectories were time-normalized with a cubic spline interpolation to allow alignment of trials. The normalized movement time was divided into ten equidistant time bins. The mean joint configuration across trials [$\mathbf{M}(t)$] was computed for each of the time bins. The joint configuration of each particular trial [$\mathbf{A}_K(t)$] was subtracted from $\mathbf{M}(t)$ for each time bin:

$$\Delta\mathbf{k}(t) = \mathbf{M}(t) - \mathbf{A}_K(t)$$

where $\Delta\mathbf{k}$ represents the deviation of the joint configuration of the kth trial from the mean joint configuration

at the end of a time bin (t). The total variance of joint configuration per degree of freedom $V_{TOT}(t)$ of the joint configuration vectors for a particular time bin was calculated as:

$$V_{TOT}(t) = \sum_{k=1}^{N} |\Delta \mathbf{k}(t)|^2 / (N \times DF)$$

where N is the total number of trials and DF is the number of degrees of freedom (i.e. the number of available joint rotations).

Partitioning of joint variance

In order to investigate how changes in joint configuration affected the hypothesized task variable, we partitioned the total joint variance per degree of freedom into two components. The first component was the uncompensated variance V_{UN}, which affected the task variable and corresponded to the variance orthogonal to the uncontrolled manifold (UCM) sub-space. The second component was the compensated variance V_{COMP}, which did not affect the hypothesized task variable and corresponded to the variance within the UCM subspace. The ratio of the two components was computed as $R_V = V_{COMP}/V_{UN}$.

Because elbow abduction–adduction and hand pronation–supination are not anatomically available in humans, we included seven joint rotations for each arm in the model to compute the total joint variance and its components: shoulder horizontal abduction–adduction, shoulder flexion–extension, shoulder inward–outward rotation, elbow flexion–extension, forearm pronation–supination, wrist flexion–extension and wrist abduction–adduction. The computational methods are described in the Appendix.

Data analysis

In addition to descriptive statistics, we applied repeated-measures ANOVA for comparisons between the pre-test and post-test. "Test" was always the within-subject factor. The between-subject factors are mentioned in every particular analysis. The number of levels of each factor is indicated as a superscript. The analysis was performed with SPSS 11 (SPSS).

Results

Kinematics

The results of the present study are based on the computed seven joint rotations of each arm. The most prominent ones in terms of the joint range of motion were horizontal abduction–adduction and inward–outward rotation in the shoulder joint, elbow flexion–extension, forearm pronation–supination and wrist flexion–extension (Fig. 3). In addition to a reduced movement time between the pre-test and post-test, Fig. 3 also illustrates the practice-associated improvement in consistency of the kinematic pattern.

When averaged across the subjects, targets and tests, the meeting point was positioned approximately 6.4 cm to the left from the midsagittal plane of the body and 55 cm in front of the sternum. A repeated-measures ANOVA ("test^2" and "target^3" being main factors) performed separately for each axis revealed significant differences in the meeting point location between all three targets along the axis Z ($F_{(2,27)} = 102.7$, $P < 0.001$; Tukey post-hoc test $P < 0.001$). No significant differences in the meeting point location (averaged across targets) between the pre-test and post-test were found for any of the axes X, Y or Z: $F_{(1,27)} = 0.1$ ($P = 0.75$), $F_{(1,27)} = 1.0$ ($P = 0.3$) and $F_{(1,27)} = 0.03$ ($P = 0.86$), respectively.

A repeated-measures ANOVA ("test^2", "target^3" and "axis^3" being main factors) was applied to the variability of the meeting point. The reduced variability (averaged across the subjects, targets and axes) from 2.3 ± 0.7 to 1.8 ± 0.7 cm (mean $\pm$ SD) between the pre-test and post-test revealed an effect of *test* ($F_{(1,81)} = 34.5$, $P < 0.001$). There was no effect of *target* ($F_{(2,81)} = 2.0$, $P = 0.14$), while the significant effect of *axis* ($F_{(2,81)} = 7.741$, $P < 0.01$, Tukey post-hoc test $P < 0.01$) suggested that the variability along the axis X was, on average, smaller than that along the axes Y and Z.

The peak velocity of the pointer and aimed target tips, and of the scalar distance between them (averaged across the subjects and targets) is presented in Fig. 4. Repeated-measures ANOVA ("test^2" and "target^3" being main factors) suggested a significant practice-associated increase in the peak velocities ($F_{(1,27)} = 6.6$, $P < 0.05$) and decrease of their variability ($F_{(1,27)} = 21.2$, $P < 0.001$; see standard deviation bars in Fig. 4).

The symmetry ratio (acceleration time/deceleration time) for the scalar distance between the pointer and aimed target tips was calculated in order to assess the relative instant of the peak velocity within the movement time. The symmetry ratio (averaged across the subjects and targets) decreased from 0.76 ± 0.2 to 0.63 ± 0.2 (mean $\pm$ SD) between the pre-test and post-test. A repeated-measures ANOVA ("test^2" and "target^3") revealed that this difference was significant ($F_{(1,27)} = 16.8$, $P < 0.001$), while there was no effect of *target* ($F_{(2,27)} = 1.46$, $P = 0.25$).

Accuracy

The overall accuracy of the pointing movement improved from the pre-test to post-test. As shown by repeated-measures ANOVA ("test^2" and "target^3"), the scalar distance between the pointer and aimed target tips significantly decreased from 13.5 ± 4.4 to 7.5 ± 2.7 cm (mean $\pm$ SD) ($F_{(1,27)} = 52.6$, $P < 0.001$), while there was no effect of *target* ($F_{(2,27)} = 2.2$, $P = 0.13$).

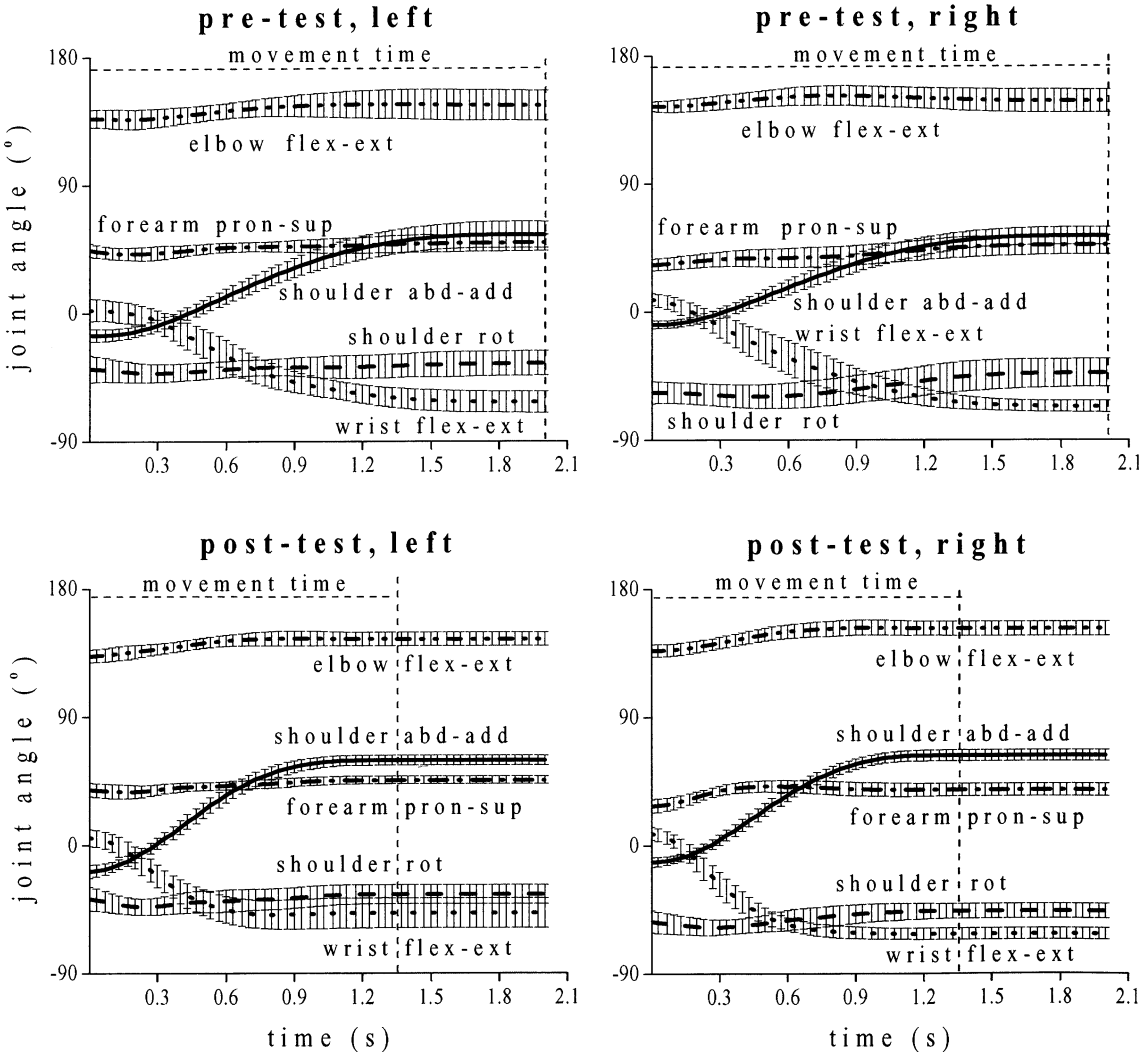

Fig. 3 Joint angles (averaged across trials) of the left (*left*) and right (*right*) arm obtained during pointing movements to the upper target in the pre-test (*upper graphs*) and post-test (*bottom graphs*) for a representative subject. Positive changes of the joint angles correspond to shoulder horizontal adduction, shoulder inward rotation, elbow extension, forearm pronation and wrist extension. The *vertical bars* represent standard deviations

In order to assess whether by the end of practice subjects were in a stable phase of the task performance we applied correlation analysis of the overall accuracy measure and trial number. The overall accuracy measure was averaged over subjects and targets for each trial (in total 20 trials per target). The correlation coefficients between the trial number and scalar distance between the pointer and aimed target tips were -0.86 ($P < 0.001$), -0.05 ($P = 0.84$) in the first and last practice sessions and -0.10 ($P = 0.68$) and -0.36 ($P = 0.12$) in the pre-test and post-test, respectively.

As shown by repeated-measures ANOVA ("test[2]", "target[3]" and "axis[3]" being main factors), the variable errors (averaged across the subjects, targets and axes) significantly decreased between the pre-test and post-test from 3.3 ± 0.9 to 2.4 ± 0.7 cm (mean $\pm$ SD) ($F_{(1,81)} = 55.0$, $P < 0.001$) (Fig. 5). The effects of *target* ($F_{(2,81)} = 11.3$, $P < 0.001$) and *axis* ($F_{(2,81)} = 36.5$, $P < 0.001$) were also significant. A Tukey post-hoc test revealed that pointing

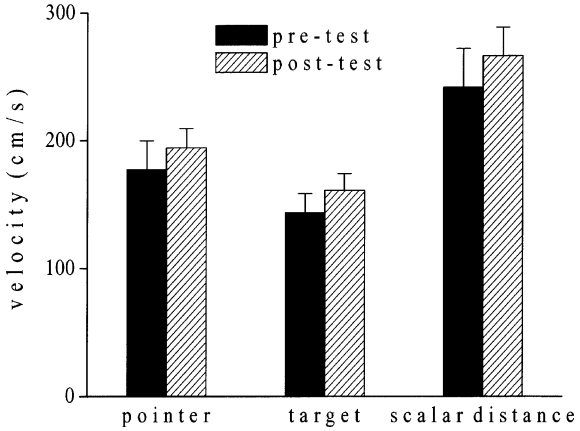

Fig. 4 Mean $\pm$ SD (averaged across trials, subjects and targets) of the peak velocity of the pointer tip, target tip, and of the scalar distance between them in the pre-test (*filled bars*) and post-test (*patterned bars*)

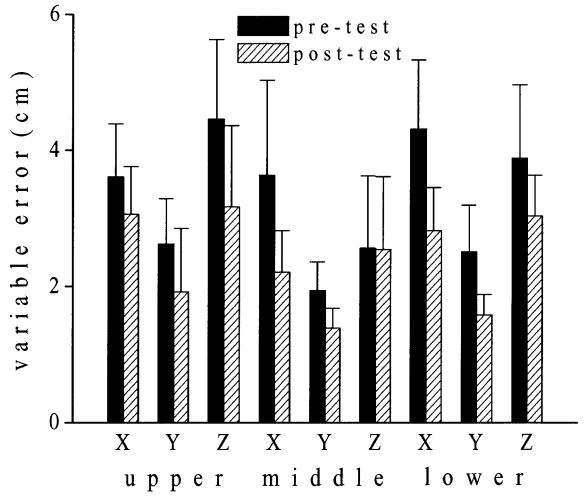

Fig. 5 Mean ± SD (averaged across the subjects) of the variable error along each axis during pointing movements to the upper, middle and lower target in the pre-test (*filled bars*) and post-test (*patterned bars*)

to the middle target was more precise than pointing to the other two targets ($P < 0.01$), while the variable errors along the axis Y were smaller than those along axes X and Z ($P < 0.001$).

Structure of joint variance

The total variance of joint configuration (V_{TOT}) per degree of freedom over the analyzed 10% bins of movement time is depicted in Fig. 6. One can notice a prominent decrease of the variance over the entire movement time between the pre-test and post-test. A repeated-measures ANOVA ("test[2]" and "target[3]") applied on the data for the joint configuration of both arms (i.e. the bimanual hypothesis), averaged across the time bins, revealed a significant decrease between the pre-test and post-test ($F_{(1,27)} = 69.8$, $P < 0.001$), but no effect of *target* ($F_{(2,27)} = 0.55$, $P = 0.6$). A repeated-measures ANOVA ("test[2]", "arm[2]" and "target[3]") applied on the data set, including data for the joint configurations of the left and right arm (i.e. the unimanual hypothesis applied to the left and right arm), averaged across the time bins, revealed a significant decrease between the pre-test and post-test ($F_{(1,54)} = 69.4$, $P < 0.001$), but neither an effect of *arm* ($F_{(1,54)} = 0.95$, $P = 0.34$) nor *target* ($F_{(1,54)} = 0.86$, $P = 0.43$). A significant interaction *test* by *arm* ($F_{(1,54)} = 5.2$, $P < 0.05$) suggested that the total variance of the right arm joint configuration reduced more from the pre-test to post-test than that of the left arm.

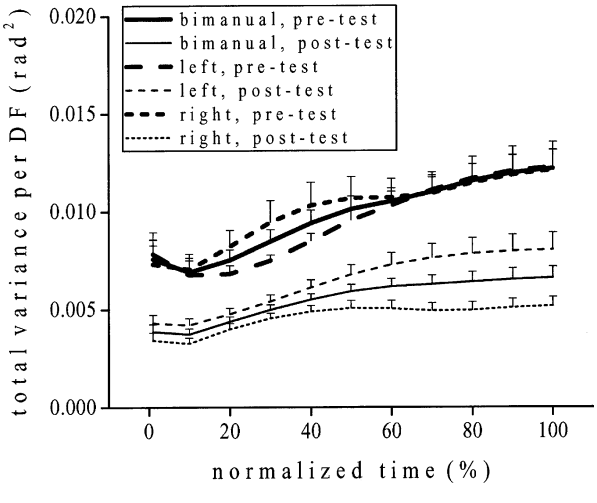

Fig. 6 Mean ± SE (averaged across the subjects and targets) of the total variance per DF (V_{TOT}) for the bimanual hypothesis and the unimanual hypothesis applied to the left and right arm, at each 10% of the normalized movement time. *Thick* and *thin lines* represent the pre-test and post-test, respectively. *Solid lines* represent the bimanual hypothesis. *Dashed* and *dotted lines* represent the unimanual hypothesis applied to the left and right arm, respectively

Figure 7 depicts the result of partitioning of the total variance into compensated (V_{COMP}) and uncompensated variance (V_{UN}), averaged across the subjects and targets for the bimanual hypothesis (Panel A), and unimanual hypothesis applied to the left (Panel B) and right (Panel C) arms. All three panels illustrate a prominent decrease in each of the variance components between the pre-test and post-test.

The data for the bimanual hypothesis, averaged across the time bins, were tested by repeated-measures ANOVA ("test[2]", "variance component[2]" and "target[3]"), where *variance component* referred to the compensated and uncompensated variance. The results revealed an effect of *test* ($F_{(1,54)} = 96.3$, $P < 0.001$) and *variance component* ($F_{(1,54)} = 154.0$, $P < 0.001$), the latter indicating that the compensated variance was significantly higher than the uncompensated variance. There was no effect of *target* ($F_{(2,54)} = 0.8$, $P = 0.45$). A significant *test* by *variance component* interaction ($F_{(1,54)} = 31.7$, $P < 0.001$) suggested that the compensated variance decreased more from the pre-test to post-test than the uncompensated variance.

The data for the unimanual hypothesis (applied to the left and right arm), averaged across the time bins, were tested by repeated-measures ANOVA ("test[2]", "variance component[2]", "arm[2]" and "target[3]"). There was a significant effect of *test* ($F_{(1,108)} = 83.5$, $P < 0.001$) and *variance component* ($F_{(1,108)} = 114.6$, $P < 0.001$), the latter suggesting that the compensated variance was significantly higher than the uncompensated variance. There were no significant effects of *arm* ($F_{(1,108)} = 0.9$, $P = 0.3$) or *target* ($F_{(2,108)} = 1.3$, $P = 0.3$). A significant interaction *test* by *arm* ($F_{(1,108)} = 5.5$, $P < 0.05$) indicated that that the averaged across components variance decreased more from the pre-test to post-test for the right arm than for the left arm. A significant interaction *test* by *variance component* ($F_{(1,108)} = 6.5$, $P < 0.05$) suggested that the compensated variance decreased more from the pre-test to post-test than the uncompensated variance.

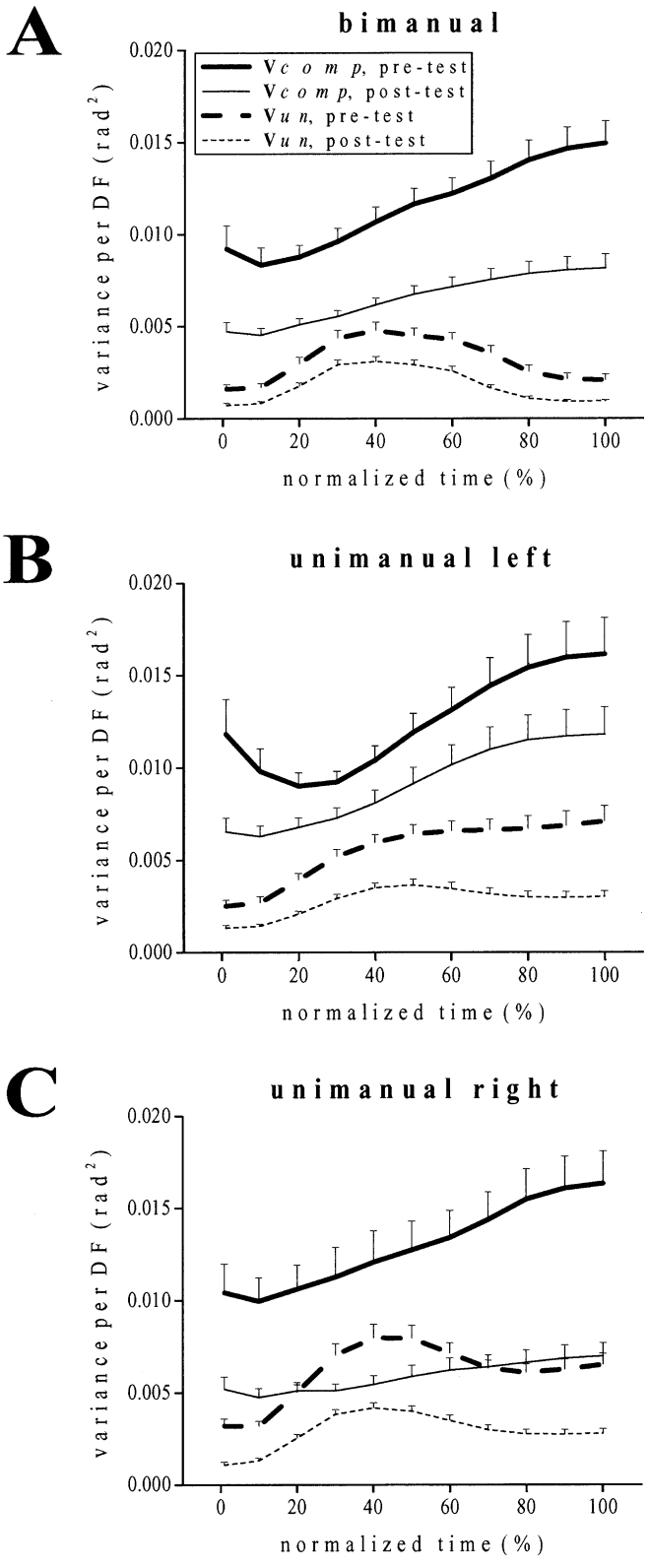

Fig. 7 Mean ± SE (averaged across subjects and targets) of the compensated (V_{COMP}) and uncompensated (V_{UN}) variance for the bimanual control hypothesis (**A**), and for the unimanual control hypothesis applied to the left arm (**B**) and to the right arm (**C**). *Thick* and *thin lines* represent the pre-test and post-test, respectively. *Solid* and *dashed lines* represent the compensated (V_{COMP}) and uncompensated (V_{UN}) variance, respectively

Finally, the ratio $R_V = V_{COMP}/V_{UN}$ was calculated over the time bins for the bimanual hypothesis and unimanual hypothesis applied to the left and right arm. The results suggest relatively high values of the ratio for the bimanual hypothesis (above 5 when averaged across the time bins and tests), while the ratio values for the unimanual hypothesis were substantially lower (Fig. 8). In addition, the ratio for the bimanual hypothesis demonstrated particularly high values during movement initiation and termination, while during the middle part of the movement the ratio was comparable with that of the unimanual hypothesis. The depicted data were averaged across the time bins and analyzed by repeated-measures ANOVA ("test^2" and "hypothesis^3"), where the *hypothesis* refers to the bimanual hypothesis and to the unimanual hypothesis applied to the left and right arm. The analysis revealed no effect of *test* ($F_{(1,27)} = 1.9$, $P = 0.18$). A prominent effect of *hypothesis* ($F_{(2,27)} = 22.3$, $P < 0.001$; Tukey post-hoc test $P < 0.001$) suggested a significantly higher ratio for the bimanual hypothesis than for the unimanual hypothesis. The ratio for the unimanual hypothesis applied to the left arm was slightly higher than that applied to the right arm, although this difference did not reach the level of significance (Tukey post-hoc test, $P = 0.07$).

Discussion

The purpose of the study was to address three predictions. With respect to the first prediction, we have shown that the general principle of UCM control is applicable to relatively unconstrained multi-effector motor tasks. Ambiguous results were obtained with respect to the second prediction—an increase in the task complexity

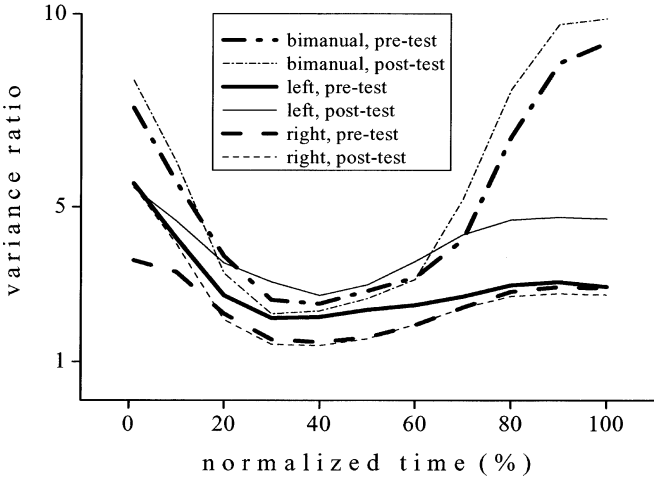

Fig. 8 Mean (averaged across subjects and targets) of the ratio $R_V = V_{COMP}/V_{UN}$ obtained within the pre-test (*thick lines*) and post-test (*thin lines*). *Dashed-dotted lines* represent the bimanual hypothesis. *Solid* and *dashed lines* represent the unimanual hypothesis applied to the left or right arm, respectively

led to no changes in the index of the UCM effect (i.e. R_V) with practice, which showed a general predicted trend (as compared with earlier studies of more simple tasks) but was short of demonstrating an increase in this effect with practice. Our observations suggest that the increased task complexity and the need to coordinate many joints was associated with a hierarchical control by the CNS, reflected in different degrees of stabilization of important performance variables by different subsets of effectors, in support of the third prediction. In the following subsections, we discuss in more detail the main findings and their implications.

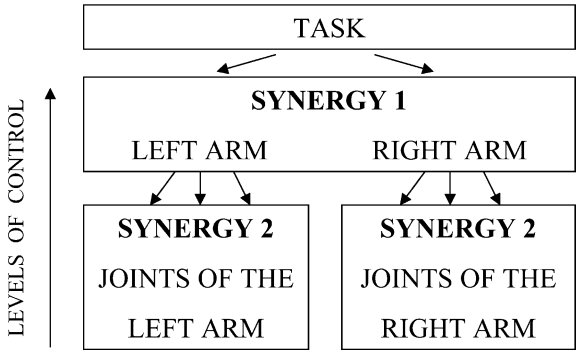

Fig. 9 Illustration of hierarchical levels of control. Synergy 1 (bimanual synergy) and Synergy 2 (synergy of joints within one arm) represent a higher and lower hierarchical levels of control, respectively

Kinematics

As compared with our previous study of bimanual pointing (Domkin et al. 2002), this study represents a repetition of the learning paradigm but applied to a more complex task. In short, the subjects were asked to practice a fast and accurate bimanual pointing over hundreds of trials separated into several sessions. Therefore, the practice-associated changes in the task-related kinematic variables could be of importance for interpreting the hypothesized practice-associated changes in the structure of joint angle variability. The main findings suggest that the subjects improved the performance of the tested movement in terms of both the movement speed and accuracy. The practice-associated improvement in accuracy in terms of variable error was similar to the improvement obtained in the previous study (Domkin et al. 2002). However, the finding that the magnitude of the variable error was twice as big as obtained previously in planar tasks (Jaric and Latash 1999; Domkin et al. 2002), suggests that employing long pointers, multiple targets and being blindfolded in the tested 3D movement indeed made the task much more difficult. The lack of a significant trend in performance (neither improvement nor worsening) in terms of overall accuracy within the last practice session and within the post-test suggested that after practice the subjects reached a stable phase in the learning of the task.

Hierarchical control of joint coordination

Some of the findings of the current study suggest that bimanual actions are controlled as a hierarchy in a sense that, at an upper level, the task is distributed between the two arms, while at a lower level the contribution of each arm is distributed among the joints (Fig. 9). This is a theoretical scheme, which cannot be currently mapped on neurophysiological structures. The analysis of the bimanual and unimanual control hypotheses produced contrasting results. Joint covariation patterns within each arm separately and within two arms working as a bimanual synergy suggested that the trajectory of the endpoint of each arm was stabilized to a much smaller degree in comparison to the vectorial distance between the arms' endpoints. We would like to offer the following explanation for this finding. During bimanual pointing success is defined by the relative motion of the two endpoints, while stabilization of the trajectories of each endpoint is less necessary. However, stabilization of stereotypical trajectories of each of the endpoints is likely to contribute to stabilization of their relative motion. Thus, for both bimanual and unimanual hypothesis the amount of joint variance per DF within the UCM subspace was larger than the amount of variance outside the UCM ($V_{COMP} > V_{UN}$). This result is similar to findings of earlier studies, which showed that joint covariation could stabilize the endpoint trajectory over a variety of tasks (Scholz and Schoner 1999; Scholz et al. 2001; Reisman et al. 2002), including bimanual pointing (Domkin et al. 2002). The latter study demonstrated that the CNS was apparently able to stabilize endpoint trajectories for a relatively simple task (planar motion and single target).

The current study made the task considerably more complex. The subjects were required to match the pointer tip with one of the three targets in three-dimensional pointing movements without vision. This task might have made it much more difficult for the CNS to elaborate stereotypical solutions for each arm for the three sub-tasks (motions to each of the three targets). When faced with a more complex task, the CNS focused predominantly on the explicit task component, i.e. making accurate pointing movements. Thus, the variance ratio R_V (quantitative index of stabilization) for the bimanual hypothesis was significantly higher than that for the unimanual hypothesis. This difference was more pronounced than that obtained in our previous study (Domkin et al. 2002). In the current study the subjects were able to covary joint rotations of both arms to stabilize a time pattern of the vectorial distance between the pointer and aimed target tips as well as to covary joint rotations within each arm to stabilize trajectory of the arm endpoint. However, the CNS clearly preferred

stabilization of the bimanual synergy at the higher hierarchical level of control (Fig. 9).

We suggest that during bimanual tasks a higher level of a control hierarchy takes responsibility for stabilization of the most relevant variable, i.e. the relative motion of the two endpoints. A lower level of the hierarchy is involved in stabilizing individual endpoint trajectories with joint angle covariation within each arm.

This explanation is similar to the conclusion of a recent study of the effects of practice on finger interaction during a complex bimanual force production task (Kang et al. 2004). The task required the subjects to produce a ramp time pattern of a task force which was computed as the sum of the forces of two asymmetrical finger pairs from each hand (for example, the index and ring fingers of the left hand and the middle and little fingers of the right hand) minus the sum of the forces produced by the remaining fingers. In that study, UCM analysis was performed using a set of hypothetical independent elemental variables, force modes (Latash et al. 2001; Scholz et al. 2002; Danion et al. 2003) to individual fingers. Prior to practice, the analysis has shown stabilization of the task force produced by the two hands by covariation of force modes to the fingers across a series of trials. However, when force modes to each finger of a hand were analyzed for each hand separately, they failed to show covariation that would stabilize the contribution of each hand to the task force.

Two stages of practice

Effects of practice on motor performance of redundant motor systems have been traditionally described as staged processes of freezing and freeing DFs (Bernstein 1967; Newell 1991; Vereijken et al. 1992; Piek 1995). The approach advocated in our study, however, claims that DFs are never eliminated (''frozen'') in the process of practice but rather their relations may be expected to get refined to stabilize important performance variables. This expectation, however, was not met in our previous study (Domkin et al. 2002), which showed a decrease in the quantitative index of stabilization (R_V) of the vectorial distance between the two endpoints in a planar bimanual task. Variance in the joint space that affected the relative distance between the endpoints (V_{UN}) dropped in the course of practice, thus, leading to more accurate performance. However, variance that did not affect the relative distance (V_{COMP}) dropped even more, such that the index of the UCM effect, R_V, decreased. This finding was interpreted as reflecting a ''floor effect'' related to over-practice of the relatively simple and partly familiar task—there was little room to decrease the joint variability orthogonal to the UCM, so the subjects used the practice to elaborate more stereotypical trajectories, possibly based on such criteria as comfort or ease of transition between movement phases.

This tentative explanation received support in a study of the effects of practice on finger interaction during a multi-finger force production task (Latash et al. 2003). That study showed a drop in variance related to important performance variables such as the total force and the total moment produced by the fingers over the first 100 trials; however, the next 100 trials brought about minimal further changes in that component of variance, while variance that did not affect either total force or total moment decreased significantly. A more recent study (Kang et al. 2004) used a complex two-hand multi-finger task and reported a significant increase in the R_V index after two days of practice.

In the current study, we tried to make the task more complex such that the subjects would not be able to easily develop stereotypical solutions. The outcome has been ambiguous. The increase in task complexity eliminated the counter-intuitive decrease in R_V described for a simpler task (Domkin et al. 2002). However, it failed to produce an increase in this index either. Maybe, to show an increase in R_V one needs to design a task that would be of an exceptional complexity (cf. Kang et al. 2004).

One should mention here a pitfall of the method for UCM analysis used in the present study, which hinders application of this method to quantify effects of practice. Hence, the current method for UCM analysis requires a set of trials, commonly 20 and more, performed under assumed unchanged control strategy. However, the subjects practice over these trials, and the UCM effect gets smudged. This method cannot detect effects of practice that occur relatively quickly, over a few trials. However, even single-trial motor learning and adaptation effects have been reported (Weeks et al. 1996; Jaric et al. 1999). Hence, the method can be applied to tasks that show steady improvement in coordination of elements over tens of trials. Recently, an alternative method has been developed for single-trial UCM analysis (Scholz et al. 2003). However, this method is currently applicable only to systems which show unchanged relationships between small changes in the outputs of the elements and changes in performance variables, i.e. unchanged Jacobian (see the Appendix) over typical trial realization. During pointing movements, the Jacobian changes with the limb geometry, making this method currently inapplicable.

We would like to conclude by suggesting that the UCM approach offers a unique and under-explored opportunity to track changes in the organization of multi-effector systems with practice. Each new study leads to partly unexpected findings that challenge the pre-existent views and suggest new questions and new experiments. This ''generative'' ability of the UCM approach is its major strength and attraction.

Acknowledgements The study was supported by grant NS-35032 from the National Institute of Health, USA, grant Nr. 208 from the University of Delaware Research Foundation (UDRF), USA and

grants from Stiftelsen för internationalisering av högre utbildning och forskning (STINT), Sweden. The authors also would like to thank two anonymous reviewers for their valuable comments and suggestions.

Appendix

Computation of variance within the uncontrolled manifold and within the orthogonal manifold

A selected task variable defines an uncontrolled manifold (UCM) in the appropriate joint space. Here we describe how the studied task variables define the corresponding UCMs at each percentage of movement time. Let $\mathbf{M}$ denote the mean joint configuration across trials. Let $\mathbf{r_0}$ be the value of the task variable for the mean joint configuration and $\mathbf{r_k}$ the value of the task variable for the kth trial. If the joint configuration vector ($\mathbf{A_k}$) of a particular trial remains in the vicinity of $\mathbf{M}$, then the deviation of the task variable $\Delta\mathbf{r_k} = \mathbf{r_k} - \mathbf{r_0}$ relates to the deviation of joint-configuration $\Delta\mathbf{k} = \mathbf{M} - \mathbf{A_k}$ approximately as:

$$\Delta\mathbf{r_k} = \mathbf{J}^*\Delta\mathbf{k} \quad (1)$$

where $\mathbf{J}$ is a Jacobian matrix. Its elements are the partial derivatives of the coordinates of the task variable with respect to the joint angles in the mean joint configuration. The nullspace of $\mathbf{J}$ represents those changes of joint configurations that do not cause any change in the task variable. The UCM is defined by this nullspace and spanned by m independent vectors (**e1,...,em**) at each instant of time. If DV is the dimension of the task variable and DF is the number of degrees of freedom of the multi-joint system, then m = DF − DV (Scholz et al. 2000).The component of Δk, which lies in the UCM, is obtained by its projection on to the nullspace. Let us denote this projection as Δk^{UCM}:

$$\Delta\mathbf{k}^{\mathrm{UCM}} = \sum_{i=1}^{m} \langle \Delta\mathbf{k},\ \mathbf{ei} \rangle * \mathbf{ei} \quad (2)$$

where < > denotes scalar product.

The component that is orthogonal to the null space is defined as:

$$\Delta\mathbf{k}^{\mathrm{ORT}} = \Delta\mathbf{k} - \Delta\mathbf{k}^{\mathrm{UCM}} \quad (3)$$

We computed the variances per DF of both components of the joint configuration vectors across N trials. The variance of the component, which lies within the UCM, is defined as compensated variance V_{COMP}:

$$V_{\mathrm{COMP}} = \sum_{k=1}^{N} \left(\Delta\mathbf{k}^{\mathrm{UCM}}\right)^2 / ((\mathrm{DF} - \mathrm{DV}) * \mathrm{N}) \quad (4)$$

The variance per DF of the orthogonal component is defined as uncompensated variance V_{UN}:

$$V_{\mathrm{UN}} = \sum_{k=1}^{N} \left(\Delta\mathbf{k}^{\mathrm{ORT}}\right)^2 / (\mathrm{DV} * \mathrm{N}) \quad (5)$$

We computed the Jacobians for the described bimanual task variable and for the unimanual task variables for each arm separately. Numerical derivation was applied for this computation.

Bimanual control hypothesis

The hypothesized task variable for the bimanual control hypothesis is the vectorial distance between the pointer tip (Px, Py, Pz) and aimed target tip (Tx, Ty, Tz). The vectorial distance is denoted by **R** = (Rx, Ry, Rz) = (Tx, Ty, Tz)−(Px, Py, Pz).

Forward kinematics was used to compute **R** from given joint angles, thus the coordinates of **R** were given as functions of 14 joint angles. The angles 1 to 7 relate to the left arm, the angles 8 to 14 relate to the right arm. The angles for the shoulder, elbow and wrist joints are described in the Methods. The joint angles (α1(t), α2(t), ..., α14(t)) and the associated vectorial distance as a function of the angles **R**(α1(t), ..., αj(t), ..., α14(t)) were given at each percentage of movement time (t = 1, ..., 100).

Let Jxj(t), Jyj(t) and Jzj(t) be the partial derivatives of Rx, Ry and Rz with respect to αj for t = 1, ..., 100.

For numerical derivation of the partial derivatives of **R** with respect to the joint angle αj we need to compute the value of **R** at the virtual joint configuration (α1(t), ..., αj(t-1), ..., α14(t)).

Note that (α1(t), ..., αj(t-1), ..., α14(t)) is a virtual joint configuration in which the jth joint angle is taken from the time bin that precedes the time bin when the other angles are considered.

Then the elements of the Jacobian are computed as the following:

$$\mathrm{Jxj}(t) = (\mathrm{Rx}(\mathrm{a1}(t),...,\mathrm{aj}(t),...,\mathrm{a14}(t)) - \mathrm{Rx}(\mathrm{a1}(t),...,\mathrm{aj}(t-1),...,\mathrm{a14}(t))) / (\mathrm{aj}(t) - \mathrm{aj}(t-1)),$$
$$\mathrm{Jyj}(t) = (\mathrm{Ry}(\mathrm{a1}(t),...,\mathrm{aj}(t),...,\mathrm{a14}(t)) - \mathrm{Ry}(\mathrm{a1}(t),...,\mathrm{aj}(t-1),...,\mathrm{a14}(t))) / (\mathrm{aj}(t) - \mathrm{aj}(t-1)),$$
$$\mathrm{Jzj}(t) = (\mathrm{Rz}(\mathrm{a1}(t),...,\mathrm{aj}(t),...,\mathrm{a14}(t)) - \mathrm{Rz}(\mathrm{a1}(t),...,\mathrm{aj}(t-1),...,\mathrm{a14}(t))) / (\mathrm{aj}(t) - \mathrm{aj}(t-1))$$

The Jacobian is a matrix with 3 rows and 14 col,umns at each instant of time:

$$\mathbf{J}(t) = \begin{matrix} \mathrm{Jx1}(t), & \mathrm{Jx2}(t), & ..., & \mathrm{Jx14}(t) \\ \mathrm{Jy1}(t), & \mathrm{Jy2}(t), & ..., & \mathrm{Jy14}(t) \\ \mathrm{Jz1}(t), & \mathrm{Jz2}(t), & ..., & \mathrm{Jz14}(t) \end{matrix}$$

The nullspace of **J** is 11-dimensional. The mean and the related deviation vectors were computed for the

lower, middle and upper target separately. The variance within the UCM for the bimanual control hypothesis was also computed for each target separately using a particular form of Eq. (4) with DF = 14 and DV = 3:

$$V_{COMP} = \sum_{k=1}^{N} \left(\Delta \mathbf{k}^{UCM}\right)^2 / (11 * N) \quad (6)$$

The variance within the orthogonal manifold was computed from Eq. (5):

$$V_{UN} = \sum_{k=1}^{N} \left(\Delta \mathbf{k}^{ORT}\right)^2 / (3 * N) \quad (7)$$

where N is the number of pointing movements (i.e. trials) to the aimed target.

Unimanual control hypothesis applied to the left and right arm

If two arms are considered separately, then the joint space for each arm is seven-dimensional. For the unimanual control hypothesis applied to the left arm the task variable is the position of the aimed target tip (Tx, Ty, Tz). For the unimanual control hypothesis applied to the right arm the task variable is the position of the pointer tip (Px, Py, Pz). Therefore, the corresponding UCMs for the left and right arm are approximated by the nullspaces of 3×7 matrices at each instant.

The elements of the Jacobian for the left and right arm are computed similarly to the computation of the Jacobian elements for the bimanual hypothesis, only using the task variables T and P instead of the vectorial distance R and seven angles of the corresponding arm instead of all 14 angles.

The nullspaces of the Jacobians for the left and right arm and thus, their UCMs are four-dimensional, while their ORTs are three-dimensional. The deviation vectors $\Delta\mathbf{k}_{\mathbf{left}}$ and $\Delta\mathbf{k}_{\mathbf{right}}$ are differences of the joint configuration of the left ($\alpha 1_k$, $\alpha 2_k$, ..., $\alpha 7_k$) or right arm ($\alpha 8_k$, $\alpha 9_k$, ..., $\alpha 14_k$) in the kth trial and the mean joint configuration of the left or right arm, respectively. The mean and the related deviation vectors were computed for the lower, middle and upper target separately. The variance per DF within the UCMs of the left and right arm can be obtained from Eq. (4) with DF = 7 and DV = 3, using $\Delta\mathbf{k}_{\mathbf{left}}$ or $\Delta\mathbf{k}_{\mathbf{right}}$, respectively. The variance within the ORTs for the left and right arm can be computed from Eq. (5) with DV = 3, using $\Delta\mathbf{k}_{\mathbf{left}}$ or $\Delta\mathbf{k}_{\mathbf{right}}$, respectively.

References

Anton H, Rorres C (2000) Elementary linear algebra: applications version. Wiley, New York

Baud-Bovy G, Soechting JF (2001) Two virtual fingers in the control of the tripod grasp. J Neurophysiol 86:604–615

Baud-Bovy G, Soechting JF (2002) Factors influencing variability in load forces in a tripod grasp. Exp Brain Res 143:57–66

Bernstein N (1935) The problem of interrelation between coordination and localization. Arch Biol Sci 38:1–35 (in Russian)

Bernstein N (1967) The co-ordination and regulation of movements. Pergamon Press, New York

Danion F, Schoner G, Latash ML, Li S, Scholz JP, Zatsiorsky VM (2003) A mode hypothesis for finger interaction during multifinger force-production tasks. Biol Cybern 88:91–98

Djupsjöbacka M, Lönn J, Olsson A (1999) A method for calibration of upper-limb kinematic data from an electromagnetic tracker system and estimation of receiver movement error. In: Herzog H, Jinha A (eds) 17th Congress of the International Society of Biomechanics, Calgary, Canada, p 218

Domkin D, Laczko J, Jaric S, Johansson H, Latash ML (2002) Structure of joint variability in bimanual pointing tasks. Exp Brain Res 143:11–23

Gelfand IM, Tsetlin ML (1966) On mathematical modeling of the mechanisms of the central nervous system. In: Gelfand IM, Gurfinkel VS, Fomin SV, Tsetlin ML (eds) Models of the structural-functional organization of certain biological systems. Nauka, Moscow, pp 9–26 (in Russian; a translation is available in 1971 edition by MIT Press, Cambridge MA)

Jaric S, Latash ML (1999) Learning a pointing task with a kinematically redundant limb: Emerging synergies and patterns of final position variability. Hum Mov Sci 18:819–838

Jaric S, Milanovic S, Blesic S, Latash ML (1999) Changes in movement kinematics during single-joint movements against expectedly and unexpectedly changed inertial loads. Hum Mov Sci 18:49–66

Kang N, Shinohara M, Zatsiorsky VM, Latash ML (2004) Learning multi-finger synergies: an uncontrolled manifold analysis. Exp Brain Res 157:336–350

Kugler PN, Kelso JAS, Turvey MT (1980) On the concept of coordinative structures as dissipative structures I. Theoretical lines of convergence. In: Stelmach GE, Requin J (eds) Tutorials in motor behavior. North Holland, Amsterdam, pp 3–45

Latash ML (1993) Control of human movement. Human Kinetics, Urbana, IL

Latash ML (1996) How does our brain make its choices? In: Latash ML, Turvey MT (eds) Dexterity and its development. Erlbaum, Mahwah, NJ, pp 277–304

Latash ML, Scholz JF, Danion F, Schoner G (2001) Structure of motor variability in marginally redundant multifinger force production tasks. Exp Brain Res 141:153–165

Latash ML, Scholz JP, Schoner G (2002) Motor control strategies revealed in the structure of motor variability. Exerc Sport Sci Rev 30:26–31

Latash ML, Yarrow K, Rothwell JC (2003) Changes in finger coordination and responses to single pulse TMS of motor cortex during practice of a multifinger force production task. Exp Brain Res 151:60–71

MacKenzie CL, Iberall T (1994) The grasping hand. North Holland, Amsterdam

Newell KM (1991) Motor skill acquisition. Annu Rev Psychol 42:213–237

Piek JP (1995) The contribution of spontaneous movements in the acquisition of motor coordination in infants. In: GlencrossDJ, Piek JP (eds) Motor control and sensory motor integration: issues and directions. Elsevier, Amsterdam, pp 199–230

Reisman DS, Scholz JP (2003) Aspects of joint coordination are preserved during pointing in persons with post-stroke hemiparesis. Brain 126:2510–2527

Reisman DS, Scholz JP, Schoner G (2002) Coordination underlying the control of whole body momentum during sit-to-stand. Gait Posture 15:45–55

Rosenbaum DA, Loukopoulos LD, Meulenbroek RGJ, Vaughan J, Engelbrecht SE (1995) Planning reaches by evaluating stored postures. Psychol Rev 102:28–67

Scholz JP, Danion F, Latash ML, Schoner G (2002) Understanding finger coordination through analysis of the structure of force variability. Biol Cybern 86:29–39

Scholz JP, Kang N, Patterson D, Latash ML (2003) Uncontrolled manifold analysis of single trials during multi-finger force

production by persons with and without Down syndrome. Exp Brain Res 153:45–58
Scholz JP, Reisman D, Schoner G (2001) Effects of varying task constraints on solutions to joint coordination in a sit-to-stand task. Exp Brain Res 141:485–500
Scholz JP, Schoner G (1999) The uncontrolled manifold concept: identifying control variables for a functional task. Exp Brain Res 126:289–306
Scholz JP, Schoner G, Latash ML (2000) Identifying the control structure of multijoint coordination during pistol shooting. Exp Brain Res 135:382–404
Seif-Naraghi AH, Winters JM (1990) Optimized strategies for scaling goal-directed dynamic limb movements. In: Winters JM, Woo SL-Y (eds) Multiple muscle systems: biomechanics and movement organization. Springer, Berlin Heidelberg New York, pp 312–334
Shim JK, Latash ML, Zatsiorsky VM (2003) Prehension synergies: trial-to-trial variability and hierarchical organization of stable performance. Exp Brain Res 152:173–184
Shinohara M, Latash ML, Zatsiorsky VM (2003) Age effects on force produced by intrinsic and extrinsic hand muscles and finger interaction during MVC tasks. J Appl Physiol 95:1361–1369
Tseng YW, Scholz JP, Schoner G, Hotchkiss L (2003) Effect of accuracy constraint on joint coordination during pointing movements. Exp Brain Res 149:276–288
Turvey MT (1990) Coordination. Am Psychol 45:938–953
Weeks DL, Aubert MP, Feldman AG, Levin MF (1996) One-trial adaptation of movement to changes in load. J Neurophysiol 75:60–74
Vereijken B, Vanemmerik REA, Whiting HTA, Newell KM (1992) Free(z)ing degrees of freedom in skill acquisition. J Mot Behav 24:133–142